06

Processes of ablation and structures growth under the action of femtosecond laser pulses on the gallium surface in an ammonia medium

© D.A. Kochuev, A.S. Chernikov, D.V. Abramov, A.A. Voznesenskaya, R.V. Chkalov, K.S. Khorkov

Vladimir State University,
Vladimir, Russia
e-mail: khorkov@vlsu.ru

Received January 17, 2023
Revised January 17, 2023
Accepted January 17, 2023

In this paper, we present the results of processing metallic gallium in an ammonia vapor medium at 2 bar pressure by femtosecond laser pulses. The influence of the ammonia concentration and the mode of laser beam scanning on the result of laser action is considered. It has been established that an increase in the concentration of ammonia vapor and a change in the scanning regime lead to a radical change in the laser ablation process. A decrease in the scanning speed leads to the cessation of the ablation process and the development of the nitridation process of the gallium surface, accompanied by the formation of columnar structures up to 12 mm long and about 100 μm in diameter. The synthesized nanoparticles and structures were studied using scanning electron microscopy, Raman spectroscopy, and X-ray analysis.

Keywords: laser ablation, gallium nitride, gallium nitride nanoparticles manufacturing, ablative synthesis of gallium nitride nanoparticles.

DOI: 10.21883/TP.2023.04.55934.4-23

Introduction

The impact of ultrashort laser radiation on materials allows their separation, changing surface properties, and producing particles having various shapes and sizes [1–7]. The use of femtosecond laser radiation for the synthesis of nanoparticles in various media is widespread [8–11]. It is this laser action that makes it possible to obtain nanoparticles of various dispersity and structure most efficiently. Laser ablation with longer pulses (longer heating time of the ionic subsystem of the target lattice, i.e. $> 10^{-10}$ s) leads to an increase in the heating area due to the thermal conductivity of the material and intense heating by the erosion laser torch [12–14]. Laser ablation of a material in a reaction medium makes it possible to form a chemical bond between the ablated material and the components of the medium, including the possibility of obtaining shell particles [15–18].

Gallium nitride (GaN) is a promising compound with high stability under radiation exposure. The characteristics of GaN-based devices are superior to those of silicon, since the average displacement energy of atoms in the lattice for GaN is 21.3 eV, which is significantly higher than that of silicon (only 11.07 eV) [19–21]. GaN devices have also found applications as elements of high-current electronics [22]. Their use as radiation sources is widespread [23], and due to its perfect chemical stability and high mobility of carriers, GaN has found its application in sensors and biosensors [24–27]. GaN materials have demonstrated biocompatibility and thus have potential applications in biomedical engineering. Biochemically tuned GaN surfaces with excellent soft tissue integration can potentially be used in various biomedical and dental applications [28–30].

In Ref. [31], the process of laser treatment of the metallic gallium surface in an ammonia environment under the action of an electrostatic field is considered. The use of this method makes it possible to obtain nanoparticles of gallium nitride and gallium oxide by ablation of metallic gallium in a reaction medium by femtosecond laser pulses [32].

The aim of this work is to study the dominant factors that determine the dynamics of the process of laser action on the surface of gallium in an ammonia medium at various thermal loads.

1. Materials and experimental technique

Gallium is a material that has a wide range of liquid state from 29.8 to 2402°C [33]; it is a rather stable chemical element, somewhat inert under normal conditions. However, changing the processing conditions and revealing the dominant factors are of great interest for studying the process of GaN formation. The use of ammonia as a working medium for the formation of GaN is due to a significantly lower ionization energy of 10.18 eV [34] compared to that of nitrogen equal to 14.53 eV [35]. The impact of laser radiation was implemented in a vessel isolated from the surrounding atmosphere.

The treatment of the metallic gallium surface was carried out according to the scheme shown in Fig. 1, where a source of femtosecond laser radiation TETA-10 (Avesta-Proekt, Troitsk, Russian Federation) was used with the following parameters: pulse duration 280 fs, pulse energy up to 150 μJ, wavelength 1030 nm, pulse repetition rate 10 kHz *1*. Scanning with a laser beam was carried out over the surface of metallic gallium *14*, located on the object table *12*,

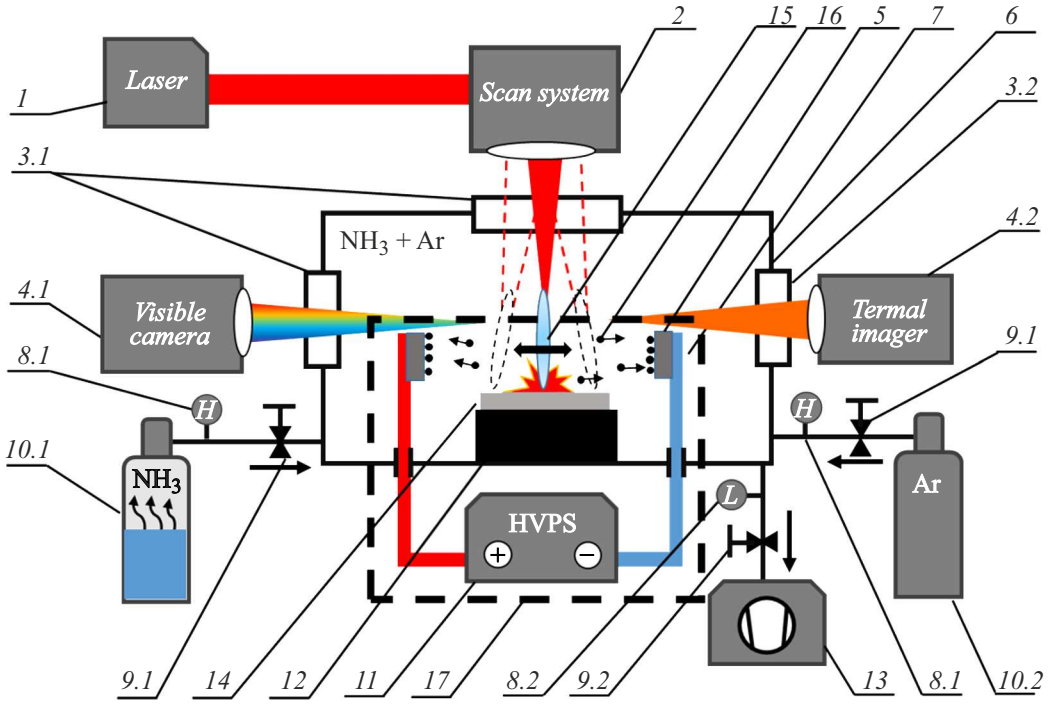

Figure 1. Scheme of the experimental setup. Explanations are given in the text.

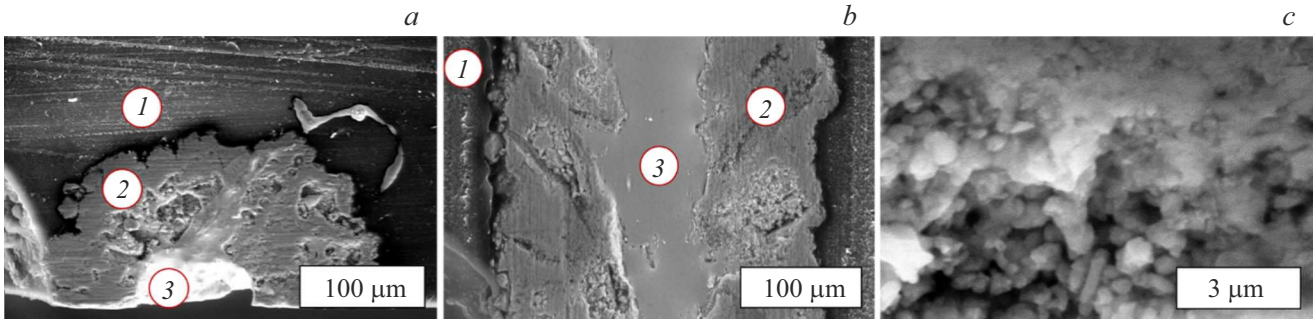

Figure 2. SEM images of the surface of a columnar structure section: transverse (*a*), longitudinal (*b*), and a magnified image of the region *2* (*c*).

with a galvanometer scanner *2* equipped with a flat field objective with a focal length of 200 mm. The input of laser radiation and the observation of processes in the visible spectral range were carried out through windows *3.1* with the appropriate antireflection coating. The speed of the laser beam scanning was 0–100 mm/s. At scanning speeds of 0–20 mm/s, melting of the processed sample was observed. In all experiments, the laser pulse energy was set at the level of 100 μJ, the diameter of the laser beam spot on the sample was 50 μm at an intensity level of $1/e^2$, and the corresponding energy flux density was 10.2 J/cm^2. Scanning with a laser beam is necessary to prevent the formation of splashes of gallium melt during the accumulation of residual heat from exposure to laser radiation and the laser erosion torch. Gallium is a fusible metal; during the formation of a bulk melt pool, a significant ejection of the liquid phase and large splashes are observed.

As a working medium, a mixture of saturated ammonia vapors obtained from a solution of 25% aqueous ammonia *10.1* and argon gas 99.998 from a vessel *10.2* was used. Before filling, the volume of the working chamber *6* was evacuated by a vacuum pump *13*. The pressure was controlled by sensors *8.1*, *8.2* and regulated by valves *9.1*, *9.2* in the range 0.1–2 bar by pumping gaseous argon, which played the role a buffer medium. The ablation products were collected using an electrostatic precipitator represented by a set of nodes *17*. The electrostatic field on the electrodes *7* was created by a source of high voltage *11* and varied in the range from *15* to 30 kV, the field strength being 2–15 kV/cm. The process of laser ablation in an electrostatic field was recorded by a camera in the visible spectral range *4.1*. The temperature was recorded through a zinc sulfide window (ZnS Multispectral) using a matrix infrared detector *4.2* with a resolution of

320 × 240, operating in the spectral range 8–14 μm *3.2*. As a result of laser action, the formation of ablated particles *16* was observed. Ablated particles under the action of the electrostatic field were deposited on the surface of silicon plates *5*, which were fixed on high-voltage electrodes. The operating principle of this approach is described in Ref. [36] for the case of solving the problem of synthesizing highly dispersed spherical powder granules by the laser ablation method. To improve the quality of the surface of the synthesized particles and to increase the process productivity, the system of ablation product collection based on an electrostatic precipitator was used directly in the area of laser beam propagation. This approach allows the formed particles to leave the laser irradiation zone without being re-exposed to the radiation source. The glow intensity from the laser-induced plasma torch *15* increased when the high voltage source was turned off, which indicates that the ablated particles re-entered the region of laser beam propagation. Carrying out ablation treatment in the isolated vessel without the electrostatic field leads to a rapid damage to the laser beam input window due to deposition of particles on the optical surface and its further degradation during the passage of the laser beam.

Temperature measurements were performed by infrared radiometry using a matrix sensor with a resolution of 320 × 240 pixels and a spectral range of 8–14 μm. Registration of thermal processes was carried out through a window made of multispectral zinc sulfide.

2. Samples study methods

Surface studies were carried out using a scanning electron microscope (SEM) (Quanta 200 3D, FEI). Images of the transverse and longitudinal sections of the resulting „columnar" structures are shown in Fig. 2, *a, b*, respectively. The transverse and longitudinal sections of the columnar structures were obtained by mechanical processing of samples embedded in epoxy resin. Mechanical processing was carried out with an abrasive tool until a section of the columnar structure was obtained in a plane corresponding to half the diameter. The obtained sections show a pronounced granular structure. The numbers indicate the zones corresponding to epoxy resin *1*, gallium nitride *2*, and metallic gallium *3*. The zones were verified using Raman spectroscopy. The magnified region of the zone *2* is shown in Fig. 2, *c*.

The Raman spectra (RS) of the synthesized columnar structures were measured in backscattering geometry using the NTEGRA Spectra probe nanolaboratory (NT-MDT, Zelenograd, Russian Federation), which is an integration of a scanning probe microscope with confocal microscopy/Raman spectroscopy. In the measurements, a diffraction grating having 1800 lines/mm was used. To study the samples, a diode-pumped solid-state laser generating radiation at a wavelength of 473 nm was used as a source of excitation.

Figure 3 shows the Raman spectra of a commercial GaN powder (Alfa Aeasar, 40218) and different areas of the surface of the synthesized columnar structure, corresponding to the SEM images. The source of excitation was laser radiation with a wavelength of 473 nm.

In the case of the Raman spectrum of commercial GaN powder (Fig. 3, *a*), peaks at frequencies 252, 418, 568, 720 cm^{-1} are clearly visible. When studying the surface and the inner part of the shell of the synthesized columnar structures (Fig. 3, *b, c*), the presence of a low-frequency wing at the high-intensity line with a frequency of 568 cm^{-1} becomes more evident. Thus, in addition to peaks at frequencies 252, 418, 568, 720 cm^{-1}, two additional peaks can be distinguished at frequencies 531 and 559 cm^{-1}. First-order modes at 531, 559, 568 and 720 cm^{-1} can be associated with phonon vibration frequencies A_1(TO), E_1 (TO), E_2(high) and A_1(LO), respectively [37]. It can be seen that the dominant bands are the E_2(high) and A_1(LO) modes centered at frequencies 568 and 720 cm^{-1}. In addition, in the case of the Raman spectrum of the inner part of the columnar structure shell (Fig. 3, *c*), the intensity of the A_1(LO) line is significantly reduced. The strong phonon line E_2(high) in the spectra reflects the characteristics of the hexagonal crystalline phase of the synthesized GaN columnar structures. Phonon modes of the second-order Raman scattering at 252 and 418 cm^{-1} (in Fig. 3, denoted by * and **) can be attributed to zone-boundary phonons activated by surface defects and finite-dimension effects [37,38]. These peaks were observed both in the case of the GaN powder and in the study of the surface and the inner part of the shell of the synthesized columnar structures. Figure 3, *d* shows the Raman spectrum

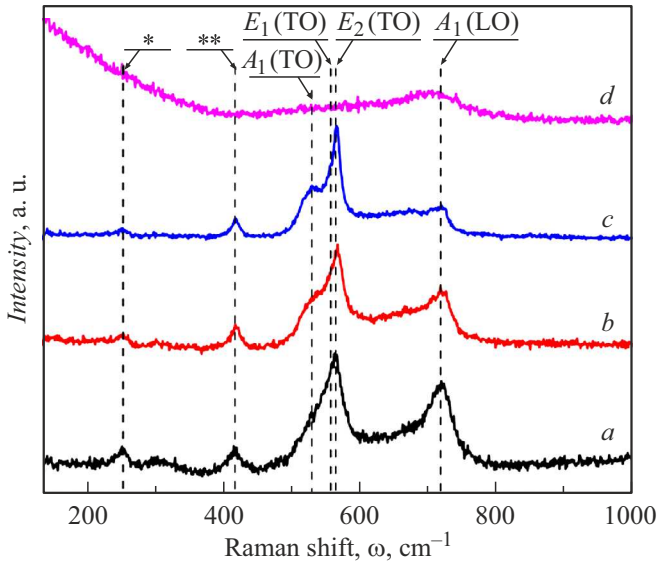

Figure 3. Raman spectra, excited by laser radiation with a wavelength of 473 nm, of the commercial GaN powder (Alfa Aeasar, 40218) *a*, the synthesized columnar structure surface *b*, the inner part of the columnar structure shell at a small distance from the central region *c*, and the central region of the columnar structure *d*.

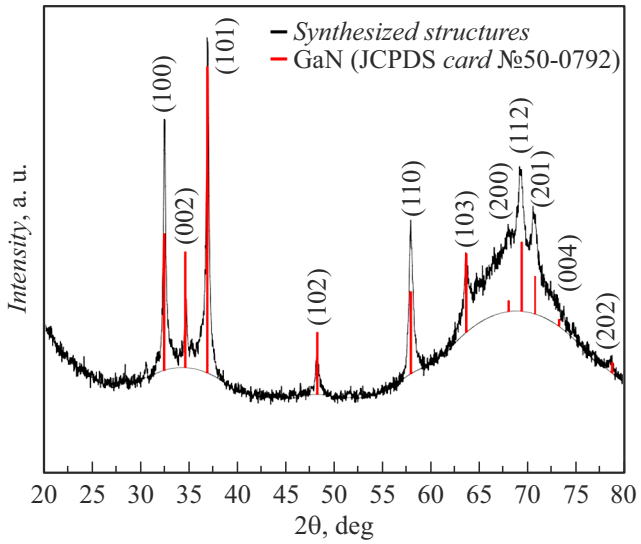

Figure 4. X-ray diffraction pattern of the synthesized columnar structures and comparison with the powder diffraction data base map (JCPDS map № 50-0792).

measured in the central region of the synthesized columnar structure (marked with *3* in Fig. 2). This region is characterized by the presence of only a melt of metallic gallium.

The structural characteristics of the synthesized columnar structures were studied by X-ray diffraction (XRD) using a D8 ADVANCE diffractometer (Bruker) with a CuK_α radiation source and a LynxEye XE detector (the measurements were carried out in the range of angles 2θ from 20 up to 80°). Figure 4 shows the diffraction pattern of the synthesized columnar structures and the corresponding map from the powder diffraction database (JCPDS map № 50-0792).

The set of diffraction peaks at 32.48, 34.55, 36.88, 47.98, 57.58, 63.50, 67.96, 69.14, 70.53, 73.41, and 78.6° corresponds to scattering by the planes of the GaN crystal lattice with the orientation (100), (002), (101), (102), (110), (103), (200), (112), (201), (004), (202), respectively. The observed peaks of the synthesized columnar structures coincide with the standard values for the GaN hexagonal wurtzite phase indicated in the powder diffraction database map JCPDS № 50-0792 (marked with red lines in the online version of Fig. 4).

3. Results and discussion

In the course of studies, a number of regularities have been established that make it possible to obtain a qualitatively different result of laser synthesis by changing the processing conditions. The most significant factors in the experiment are the laser beam scanning mode and ammonia concentration. The use of an electrostatic field makes it possible to remove ablated particles from the region of laser radiation propagation, and the pressure in the working vessel was controlled using argon.

Surface treatment of gallium using vapors of 25% aqueous ammonia solution as a reaction medium makes it possible to obtain spherical nanoparticles of gallium, gallium nitride and oxide. The presence of gallium particles, including gallium oxides in the obtained materials, indicates an insufficient energy impact during laser ablation. For ablated particles, the conditions for nitrogen sorption and GaN formation are not created, which is probably due to insufficient time of being at the temperature required for GaN formation. These conditions can be formed by increasing the energy of the laser erosion torch and the laser-induced plasma channel, which was proposed in Refs. [39,40]. These methods can effectively control the processes of heating, expansion of nanoparticles, and the time of their stay in the high temperature region.

Changing the scanning speed allows adjusting the intensity of ablation, as well as the size of the fraction of the resulting particles. The use of a scanning speed of up to 100 mm/s leads to an abundant ejection of the liquid phase of the material onto the surface of the substrates. This is a consequence of the reactive action of the laser erosive torch and the vapor-gas channel formed during the laser impact. Increasing the scanning speed makes it possible to obtain ablated nanoparticles without splashes of metallic gallium and reduce the overall energy exposure to the affected area. In this case, a lower heating of the surface and a decrease in the ablation effect of the laser beam are observed.

Under laser action on the surface of liquid gallium in a medium of saturated vapor obtained by evaporation of 25% of aqueous ammonia, with a scanning speed of more than 100 mm/s, an intense ablation process is observed. The inner space of the chamber is filled with ablated particles, which, under the action of the electrostatic field, are collected into filamentous structures that line up along the lines of the field strength. A reduction in the scanning speed of the laser beam to values below 20 mm/s leads to a significant decrease in the intensity of the ablation process. The result of laser exposure is the formation of an „island structure“ on the surface of the sample. The Raman spectrum of the island structure surface coincides with the spectrum of the inner part of the shell of the columnar structure (Fig. 3, *c*). The similarity of the recorded spectra of the regions is due to the temperature regime of formation. An increase in temperature facilitates the development of the GaN crystalline phase, whose Raman spectra coincide with those of the commercial powder. During the formation of island structures, these temperature conditions are not achieved. A microphotograph of the process obtained with a CCD camera is shown in Fig. 5. The dashed arrow indicates the region of the formed island structure on the surface of liquid gallium. During the laser beam action on the sample surface, its melting is observed and due to the forces of surface tension, a near-spherical surface is formed. In the laser beam impact zone, a meniscus is formed due to a local increase in pressure (reactive

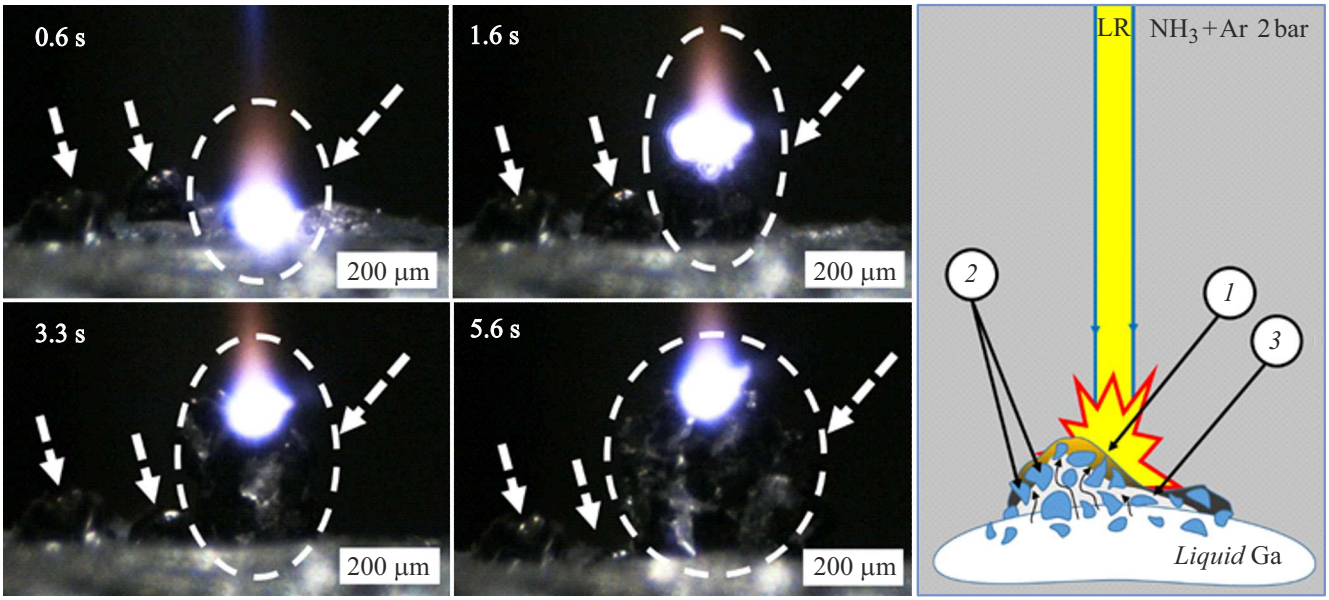

Figure 5. The process of formation of an island structure on the surface of liquid gallium: *1* — area of laser beam impact, *2* — GaN, *3* — base of the columnar structure.

action of the laser erosion torch). The area affected by the laser beam has a pronounced laser erosion torch, growing together with the laser-induced plasma channel. The glow intensity is determined by the interaction of laser radiation with gallium vapor and ammonia. The sample surface temperature in the ablation treatment mode, including the island structure formation mode, does not exceed 39°C, the temperature of the formed island structures corresponds to 240−270°C.

The single-point action of laser radiation on the surface of gallium in an ammonia vapor medium leads to the formation of „columnar structures“ (Fig. 6). The intensity of the laser erosion torch and the laser-induced plasma channel noticeably decreases, which is associated with the transition from the ablation regime to the regime of columnar structure growth. Significant changes in the sample surface temperature are observed, reaching 220−330°C. The increase in the recorded temperature in this regime of exposure is probably associated with the deterioration of thermal contact with the surface of the object stage due to drift over the surface of liquid gallium.

Further exposure to laser radiation leads to the formation of columnar structures in the direction of the laser beam action (Fig. 6, *c*). The growth of such structures proceeds most intensively at a height of more than 0.7−1 mm from the gallium sample surface. Intensive heating of the affected area is also observed. The temperature in the affected area (growth zone) is 870−1020°C. Significant deviations in the temperature data are caused by the instability of the growing structure position. At its base, there is liquid gallium. In the process of growth, fluctuations of the structure by the order of 100−150 μm are observed. The temperature was recorded using an infrared camera that records the process from one position.

Figure 7 illustrates the columnar structure growth with an interval of 0.3 s. When the structure is deflected towards the camera, the action of the laser beam occurs from the opposite side, and a lower temperature is recorded. When the columnar structure deviates in the direction „from the camera“, the area directly exposed to the laser beam is recorded, which corresponds to the maximum recorded temperature.

These structures can be formed as a result of the formation of GaN grains. Crystallization occurs as a result of nitrogen sorption during the dissociation of ammonia from the surrounding atmosphere. Further heating of the affected area promotes the growth of the GaN grain. The vertical growth of the observed structures occurs as a result of a cycle of events, namely, the formation of GaN crystals, the formation of capillary flows of liquid metal between the crystals, including those over the surface of the resulting structure, the growth of GaN crystals as a result of laser heating of the bulk material and the interaction of gallium with nitrogen (ammonia dissociated in the presence of gallium). The growth of crystals during heating by laser radiation contributes to a decrease in the size of the capillary, which, in turn, contributes to an increase in the potential height of the capillary flow (due to a decrease in the mass of the liquid metal column) and intensification of growth, which is schematically shown in Fig. 6, *b*.

As a result, the dominant effect of the reaction medium on the laser treatment process was established. The use of aqueous ammonia with a concentration of 25% as a source of saturated ammonia vapors, the reaction medium in the process of laser exposure, contributes to an increase in the intensity of the ablation action along with the yield of nanoparticles.

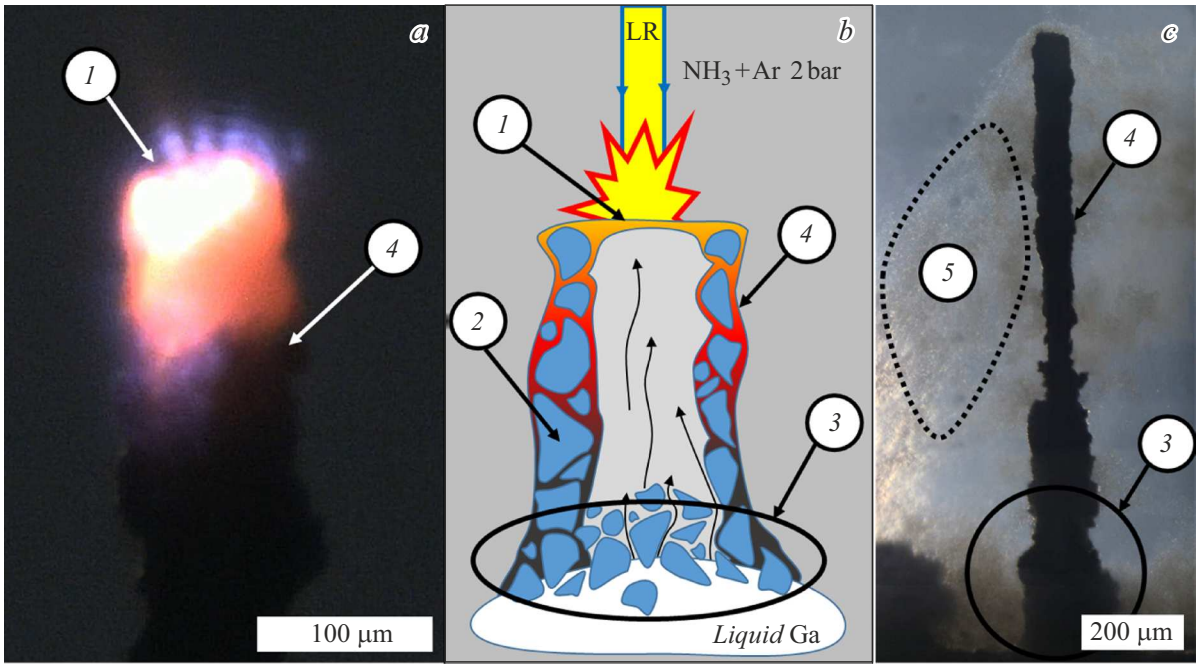

Figure 6. Columnar structure growth process: *1* — laser beam impact region, *2* — GaN, *3* — columnar structure base/island structure, *4* — columnar structure, *5* — filamentous structures.

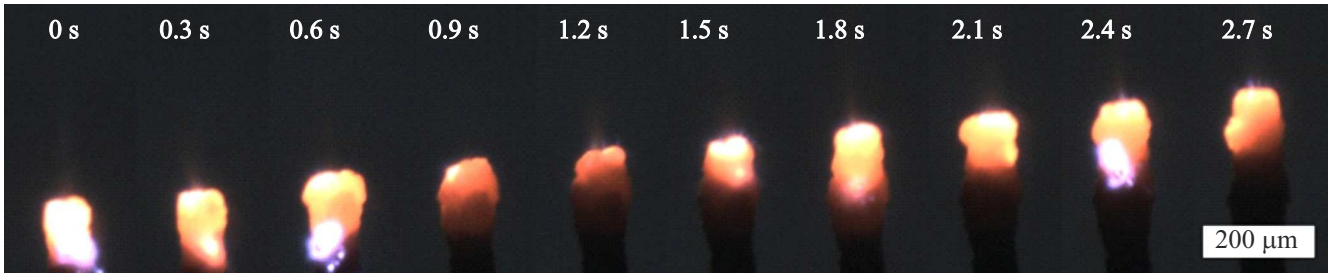

Figure 7. The process of columnar structure growth with a CCD camera shooting rate of 0.3 s (the diameter of the columnar structure is 100 μm).

Reducing the processing speed makes it possible to obtain structures whose growth is directed towards the action of the laser beam. This method makes it possible to obtain bulk structures from polycrystalline GaN. The growth productivity is about 150 μm/s with a columnar structure diameter of about 100 μm and a length of up to 12 mm. The instability of the geometry of the resulting columnar structures is caused by vibrations of the rod during the laser action.

The obtained columnar structures are the result of the formation of GaN grains and nanoparticles of various shapes and sizes, which can be seen in Fig. 2, *c*. Examples of the formation of such structures by chemical vapor deposition are considered in the review [41]. Based on the analysis of the achieved characteristics, it is proposed to use them in the production of LEDs, piezoelectric nanogenerators, photovoltaic devices, devices for photocatalytic water splitting, and in biologic applications. The obtained structures can also be used as targets for laser ablative synthesis of spherical GaN nanoparticles. It should be noted that the rate of the laser-induced formation of structures considered in this paper is much higher than in the case of using the chemical vapor deposition method.

Conclusion

In this paper, we studied the mechanisms of interaction of laser radiation with a gallium surface in an ammonia medium. Within the framework of this study, we investigated the effect of scanning speed on the result of processing and the nature of the gallium nitride formation reaction. The considered method for obtaining gallium nitride in the form of nanoparticles or columnar structures has its own competitive advantages compared to the classical methods. The properties characteristic for this method include the dynamics of the gallium nitride synthesis, both bulk structures and nanomaterials. These

results can also be applied to the formation of ordered micro- and nanostructures on a surface containing metallic gallium upon treatment in ammonia with sharply focused laser radiation. When using microscopic objectives, it is possible to reduce the size of the affected area by a factor of two, as well as to reduce the heating zone of the laser beam, and, as a result, to obtain smaller-scale structures.

Funding

The study of the processes of formation of nanoparticles was supported by the Russian Science Foundation (grant № 22-79-10348). The preparation and analysis of samples was carried out within the framework of the State Assignment of the Ministry of Science and Higher Education of the Russian Federation, topic FZUN-2020-0013.

Conflict of interest

The authors declare that they have no conflict of interest.

References

[1] M.V. Shugaev, C. Wu, O. Armbryster, A. Naghilou, N. Brouwer, D.S. Ivanov, T.J.-Y. Derrien, N.M. Bulgakova, W. Kautek, B. Rethfeld, L.V. Zhigilei. MRS Bulletin, **41** (12), 960 (2016). DOI: 10.1557/mrs.2016.274
[2] A.A. Ionin, S.I. Kudryashov, A.A. Samokhin. Phys. Usp., **60**, 149 (2017). DOI: 10.3367/UFNe.2016.09.037974
[3] R. Fedorov, F. Lederle, M. Li, V. Olszok, K. Wöbbeking, W. Schade, E.G. Hübner. Chem. Plus. Chem., **86** (9), 1231 (2021). DOI: 10.1002/cplu.202100118
[4] J. Hao, S. Xu, B. Gao, L. Pan. Nanomaterials, **10** (3), 439 (2020). DOI: 10.3390/nano10030439
[5] J. Perriére, C. Boulmer-Leborgne, R. Benzerga, S. Tricot. J. Phys. D: Appl. Phys., **40** (22), 7069 (2007). DOI: 10.1088/0022-3727/40/22/031
[6] V.V. Osipov, V.V. Platonov, A.M. Murzakaev, E.V. Tikhonov, A.I. Medvedev. Kvant. elektron., **52** (8), 739 (2022) (in Russian).
[7] J.L.H. Chau, C.Y. Chen, M.C. Yang, K.L. Lin, S. Sato, T. Nakamura, C.C. Yang, C.W. Cheng. Mater. Lett., **65** (4), 804 (2011). DOI: 10.1016/j.arabjc.2013.04.014
[8] A.V. Kabashin, M. Meunier. J. Appl. Phys., **94** (12), 7941 (2003). DOI: 10.1063/1.1626793
[9] A.A. Popov, G.V. Tikhonowski, P.V. Shakhov, E.A. Popova-Kuznetsova, G.I. Tselikov, R.I. Romanov, A.M. Markeev, S.M. Klimentov, A.V. Kabashin. Nanomaterials, **12** (10), 1672 (2022). DOI: 10.3390/nano12101672
[10] K.S. Khorkov, D.V. Abramov, D.A. Kochuev, S.M. Arakelian, V.G. Prokoshev. Phys. Proced., **83**, 182 (2016). DOI: 10.1016/j.phpro.2016.08.152
[11] P.A. Danilov, A.A. Ionin, S.I. Kudryashov, A.A. Rudenko, I.N. Saraeva, D.A. Zayarny. Las. Phys. Lett., **14** (5), 056001 (2017). DOI: 10.1088/1612-202X/aa6225
[12] B.N. Chichkov, C. Momma, S. Nolte, F. Von Alvensleben, A. Tünnermann. Appl. Phys. A, **63** (2), 109 (1996). DOI: 10.1007/BF01567637
[13] S. Nolte, C. Momma, H. Jacobs, A. Tünnermann, B.N. Chichkov, B. Wellegehausen, H. Welling. JOSA B, **14** (10), 2716 (1997). DOI: 10.1364/JOSAB.14.002716
[14] G.N. Makarov. Phys. Usp., **56**, 643 (2013). DOI: 10.3367/UFNe.0183.201307a.0673
[15] A.S. Chernikov, D.A. Kochuev, A.A. Voznesenskaya, A.V. Egorova, K.S. Khorkov. J. Phys.: Conf. Ser., **2077** (1), 012002 (2021). DOI: 10.1088/1742-6596/2077/1/012002
[16] G.I. Tselikov, G.A. Ermolaev, A.A. Popov, G.V. Tikhonowski, D.A. Panova, A.S. Taradin, A.A. Vyshnevyy, A.V. Syuy, S.M. Klimentov, S.M. Novikov, A.B. Evlyukhin, A.V. Kabashin, A.V. Arsenin, K.S. Novoselov, V.S. Volkov. Proc. Natl. Acad. Sci. USA, **119** (39), e2208830119 (2022). DOI: 10.1073/pnas.2208830119
[17] J. Simon, V.P.N. Nampoori, M. Kailasnath. Optik, **195**, 163168 (2019). DOI: 10.1016/j.ijleo.2019.163168
[18] D.A. Kochuev, K.S. Khorkov, A.V. Ivashchenko, V.G. Prokoshev, S.M. Arakelian. J. Phys. Conf. Ser., **951** (1), 012015 (2018). DOI: 10.1088/1742-6596/951/1/012015
[19] P. Hazdra, S. Popelka. Phys. Status Solidi A, **214** (4), 1600447 (2017). DOI: 10.1002/pssa.201600447
[20] K. Li, P.L. Evans, C.M. Johnson. IEEE Trans. Power Electron., **33** (6), 5262 (2017). DOI: 10.1109/TPEL.2017.2730260
[21] V.K. Pandey, C.M. Tan. IEEE Trans. Nucl. Sci., **68** (6), 1319 (2021). DOI: 10.1109/TNS.2021.3072654
[22] B.J. Baliga. Semicond. Sci. Technol., **28** (7), 074011 (2013). DOI: 10.1088/0268-1242/28/7/074011
[23] R. Quay. *Gallium Nitride Electronics* (Springer, Heidelberg, 2008) DOI: 10.1007/978-3-540-71892-5
[24] C.M. Furqan, M.U. Khan, M. Awais, F. Jiang, J. Bae, A. Hassan, H.S. Kwok. Sci. Rep., **11** (1), 1 (2021). DOI: 10.1038/s41598-021-89956-0
[25] D. Han, Y. Chen, D. Li, H. Dong, B. Xu, X. He, S. Sang. Sens. Actuators B Chem., **379**, 133197 (2023). DOI: 10.1016/j.snb.2022.133197
[26] J. Zhou, H. Huang, M. Wang, D. Zhao, J. Yu, S. Jin, Y. Zhong, X. Chen, X. Yu, P. Liu, J. Zhao. Sens. Actuators B Chem., **345**, 130360 (2021). DOI: 10.1016/J.SNB.2021.130360
[27] K. Asha, A. Sanjana, K. Narayan. In: *2018 2nd International Conference on Trends in Electronics and Informatics* (Tirunelveli, India, 2018), p. 955. DOI: 10.1109/ICOEI.2018.8553909
[28] S. Cojocari, O. Ignatov, M. Jian, V. Cobzac, T. Braniste, E.V. Monaico, A. Taran, V. Nacu Int. J. Biomed. Eng. Technol. Springer, Cham (Moldova, 2021), p. 373. DOI: 10.1007/978-3-030-92328-0_49
[29] N. Wazzan, K.A. Soliman, W.S. Abdel Halim. J. Mol. Model., **25** (9), 1 (2019). DOI: 10.1007/s00894-019-4147-8
[30] M. Mishra, J. Sharan, V. Koul, O.P. Kharbanda, A. Kumar, A. Sharma, T.A. Hackett, R. Sagar, M.K. Kashyap, G. Gupta. Appl. Surf. Sci., **612**, 155858 (2023). DOI: 10.1016/j.apsusc.2022.155858
[31] D.A. Kochuev, A.S. Chernikov, R.V. Chkalov, A.V. Prokhorov, K.S. Khorkov. J. Phys. Conf. Ser., **2131** (5), 052089 (2021). DOI: 10.1088/1742-6596/2131/5/052089
[32] A.S. Chernikov, D.A. Kochuev, R.V. Chkalov, A.V. Egorova, D.G. Chkalova. *2022 International Conference Laser Optics* (Saint Petersburg, Russian Federation, 2022), p. 1. DOI: 10.1109/ICLO54117.2022.9840086
[33] R.R. Moskalyk. Miner. Eng., **16** (10), 921 (2003). DOI: 10.1016/j.mineng.2003.08.003

[34] P. Limão-Vieira, N.C. Jones, S.V. Hoffmann, D. Duflot, M. Mendes, A.I. Lozano, F. Ferreira da Silva, G. Garcia, M. Hoshino, H. Tanaka. J. Chem. Phys., **151** (18), 184302 (2019). DOI: 10.1063/1.5128051
[35] A. Kramida, Yu. Ralchenko, J. Reader and NIST ASD Team (2022). NIST Atomic Spectra Database (ver. 5.10), [Online]. Available: https://physics.nist.gov/asd [2022, December 29]. National Institute of Standards and Technology, Gaithersburg, MD.
[36] D.A. Kochuev, A.S. Raznoschikov, R.V. Chkalov. IOP Conf. Ser.: Mater. Sci. Eng., **969** (1), 012034 (2020). DOI: 10.1088/1757-899X/969/1/012034
[37] C.C. Chen, C.C. Yeh, C.H. Chen, M.Y. Yu, H.L. Liu, J.J. Wu, K.H. Chen, L.C. Chen, J.Y. Peng, Y.F. Chen. J. Am. Chem. Soc., **123** (12), 2791 (2001). DOI: 10.1021/ja0040518
[38] E. Li, S. Song, D. Ma, N. Fu, Y. Zhang. J. Electron. Mater., **43** (5), 1379 (2014). DOI: 10.1007/s11664-014-3079-4
[39] A.S. Chernikov, D.A. Kochuev, A.A. Voznesenskaya, A.V. Egorova. J. Phys. Conf. Ser., **1942** (1), 012024 (2021). DOI: 10.1088/1742-6596/1942/1/012024
[40] D.A. Kochuev, A.F. Galkin, A.A. Voznesenskaya, K.S. Khorkov, R.V. Chkalov. Bull. Lebedev Phys. Inst., **47** (2), 372020 (2020). DOI: 10.3103/S1068335620020062
[41] Yu. Lan, J. LI, W. Wong-Ng, R.M. Derbeshi, J. Li, A. Lisfi. Micromachines, **7** (9), 121 (2016). DOI: 10.3390/mi7090121

Translated by Ego Translating